

Hierarchical Mixture of Experts: Generalizable Learning for High-Level Synthesis

Weikai Li, Ding Wang, Zijian Ding, Atefeh Sohrabizadeh, Zongyue Qin,
Jason Cong, Yizhou Sun

University of California, Los Angeles
weikaili@cs.ucla.edu, allenwang2333@gmail.com, {bradyd, atefehsz, qinzongyue, cong, yzsun}@cs.ucla.edu

Abstract

High-level synthesis (HLS) is a widely used tool in designing Field Programmable Gate Array (FPGA). HLS enables FPGA design with software programming languages by compiling the source code into an FPGA circuit. The source code includes a program (called “kernel”) and several pragmas that instruct hardware synthesis, such as parallelization, pipeline, etc. While it is relatively easy for software developers to design the program, it heavily relies on hardware knowledge to design the pragmas, posing a big challenge for software developers. Recently, different machine learning algorithms, such as GNNs, have been proposed to automate the pragma design via performance prediction. However, when applying the trained model on new kernels, the significant domain shift often leads to unsatisfactory performance. We propose a more domain-generalizable model structure: a two-level hierarchical Mixture of Experts (MoE), that can be flexibly adapted to any GNN model. Different expert networks can learn to deal with different regions in the representation space, and they can utilize similar patterns between the old kernels and new kernels. In the low-level MoE, we apply MoE on three natural granularities of a program: node, basic block, and graph. The high-level MoE learns to aggregate the three granularities for the final decision. To stably train the hierarchical MoE, we further propose a two-stage training method. Extensive experiments verify the effectiveness of the hierarchical MoE.

Introduction

With the heated demand for domain-specific accelerators, field-programmable gate arrays (FPGA) are widely used. It is, however, labor-intensive to write register-transfer-level hardware description languages, such as VHDL and Verilog. High-level synthesis (HLS) provides a much easier solution by compiling a source code written in a software programming language, such as C, MatLab, etc., into an FPGA circuit (Cong et al. 2011, 2022; Schafer and Wang 2019).

The source code consists of a program (also called “kernel”) that describes the FPGA’s functional behaviors, and several pragmas inserted in the program that instruct the hardware synthesis process, such as parallelization, pipeline, etc., as illustrated in the code snippets in Fig. 1. While it is relatively easy to design the program, it heavily requires hardware knowledge to design the pragmas, and different

pragma designs can lead to significantly different FPGA performances, posing a great challenge for software developers (Sohrabizadeh et al. 2022). Recent works have automated pragma design for programs, employing heuristics methods or machine learning methods. The heuristic methods use bottleneck analysis (Sohrabizadeh et al. 2021) or non-linear programming based on lower-bound objective function (Pouget, Pouchet, and Cong 2024a,b). The machine learning methods train a surrogate model to predict the FPGA’s performance from the source code, so that we can rely on the model prediction to find the best pragmas without running time-consuming HLS. Since HLS data is very scarce, it is difficult to train a large language model, and graph neural networks (GNNs) that are based on the control data flow graph (Sohrabizadeh et al. 2022; Bai et al. 2022; Sohrabizadeh et al. 2023; Ustun et al. 2020; Wu, Xie, and Hao 2023; Wu et al. 2022a) are widely utilized. Some very recent work (Qin et al. 2024) explores using both GNN and lightweight language models.

While machine learning models have better learning ability than the heuristic methods, they do not generalize well to unseen kernels. In real-world applications, we often encounter new circuit design requirements. The model trained on existing kernels usually fails to perform well on new kernels. This can be viewed as a domain generalization (Bai et al. 2022; Kwon and Carloni 2020) problem, where each kernel is a domain. Note it is very time-consuming to run HLS to acquire the labels on new kernels, with each run taking minutes to hours (Sohrabizadeh et al. 2023), thus data-efficient fine-tuning is required for new kernels. Domain generalization methods for GNN usually employ adversarial training to align the representation space between the source domain and target domain (Dai et al. 2019; Zhang et al. 2019; Wu et al. 2020; Shen et al. 2023), or do data augmentation to learn invariant representation under risk extrapolation (Wu et al. 2022b; Liu et al. 2023a). However, these approaches are not applicable to our application, as the differences between kernels are informative for the prediction, so forcing them to the same distribution does not work.

Nonetheless, a unique opportunity of the HLS prediction task is that kernels usually share some similar substructures, as shown in Fig. 1. It could be beneficial if we can leverage such similarities. We thus propose a two-level hierarchical mixture of experts (MoE) to address this issue. MoE (Ja-

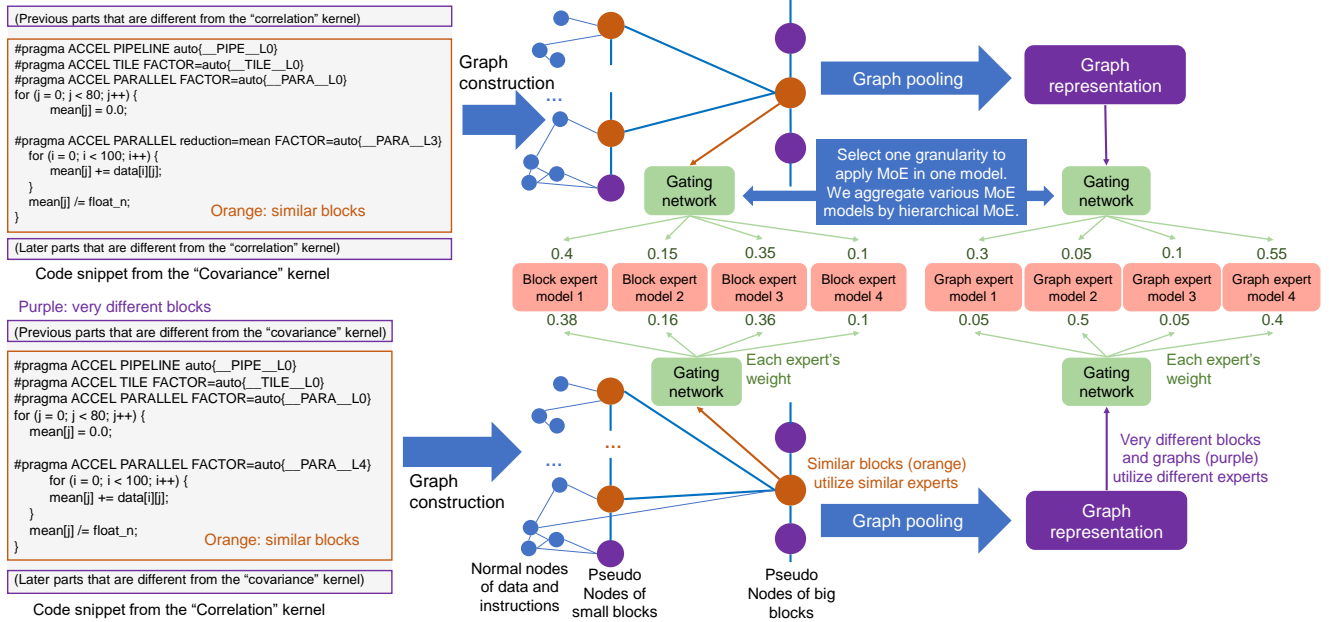


Figure 1: Motivation of utilizing MoE. The two kernels share a similar nested loop, while they are different in codes outside this screenshot. Similar blocks/graphs can utilize similar experts via similar gating, while different blocks/graphs can utilize different experts.

cobs et al. 1991; Shazeer et al. 2017) uses several expert networks instead of a single fixed network, and it computes the weighted sum of their outputs. Different experts can specialize in different regions in the hidden representation space, so that similar substructures in different domains can be processed by the same expert. A gating network computes the expert assignment, which learns to discern which expert should deal with which substructure. GraphMETRO (Wu et al. 2024) applies MoE to improve GNN’s generalizability by predefining a set of domain shifts and training each expert to deal with one type of domain shift by data augmentation. We take an orthogonal direction, eliminate the need for hardware knowledge to define the domain shifts, and focus on the model structure rather than data augmentation.

While designing the model architecture is nontrivial, another unique opportunity for HLS prediction is that the input graph naturally has three granularities: nodes, blocks, and the whole graph. MoE can be constructed on either of these three granularities. Then, which granularity to choose? It is a hard task as each kernel might benefit from different granularities differently. Simply applying MoE on all three granularities in one model does not work. Therefore, we propose a higher-level MoE to aggregate the three low-level MoEs according to the need. Nonetheless, optimization with the hierarchical MoE is challenging. Since the three low-level MoEs are different, training easily leads to expert polarization. We propose a two-stage training and constant initialization to stabilize the training. To the best of our knowledge, while some papers (Shazeer et al. 2017) have studied hierarchical MoE to improve memory efficiency, this is the first study that demonstrates the performance gain of hierarchical MoE, and it might also potentially benefit other applica-

tions. We conduct extensive experiments on the largest HLS benchmark dataset, HLSyn (Bai et al. 2023), and the experiment results reveal the effectiveness of hierarchical MoE. In summary, we make the following contributions:

- We identify the difficulties of domain generalizable learning in HLS prediction and formalize this problem.
- We propose the hierarchical MoE to address these challenges, and a two-stage training to stabilize its training.
- Extensive experiments verify the effectiveness of our methods, where the average speedup of the FPGA design is 26.6% higher than that of the baseline method.

Related Work

Machine Learning for HLS Prediction

There are two research directions for HLS pragma design automation. The first direction is heuristic-driven. AutoDSE (Sohrabizadeh et al. 2021) uses bottleneck-guided searching based on the feedback from the HLS report, and it is well-generalizable. Non-linear programming performs well on affine kernels based on a lower-bound objective function (Pouget, Pouchet, and Cong 2024a,b). The second direction is data-driven, which trains a surrogate machine learning model to predict the FPGA’s performance. GNNs (Sohrabizadeh et al. 2022, 2023; Ustun et al. 2020; Wu et al. 2022a; Wu, Xie, and Hao 2023, 2021; Qin et al. 2024) are widely used. While machine learning models could perform better than heuristic methods with sufficient training data, they suffer from poor generalizability. To solve this issue, previous works use meta-learning method, MAML (Finn, Abbeel, and Levine 2017), to find a generalizable parameter initialization (Bai et al. 2022), or train a

separate domain adaptor for each domain (Kwon and Carloni 2020). They perform well in some situations, but in our case, we have too many kernels to stably train MAML, and we only have hundreds of data for each kernel, so it is difficult to train an individual adaptor. Instead, we explore an orthogonal direction of improving the generalizability of the model structure.

Domain Generalization for Graph Neural Network

Domain generalization aims to reduce the performance gap between the source domains and target domains. Most related works (Dai et al. 2019; Zhang et al. 2019; Wu et al. 2020; Shen et al. 2023) employ adversarial training to align the representation space between the source and target domains. Some papers (Wu et al. 2022b; Liu et al. 2023a) design specific data augmentation methods and learn invariant representations under risk extrapolation. However, we cannot directly align the representation space of different kernels since their difference is large and informative. GraphMETRO (Wu et al. 2024) predefines several types of domain shifts and uses MoE to deal with them, where each expert deals with one type of domain shift. While it is a good general method, we take an orthogonal direction and eliminate the need for extensive hardware knowledge to define the domain shifts, and our model based on the three granularities is specifically designed for the HLS prediction task.

Mixture of Experts (MoE)

MoE trains several expert networks and calculates the weighted sum of their outputs (Jacobs et al. 1991; Shazeer et al. 2017). It is useful in domain transfer learning in computer vision (Li et al. 2023; Zhong et al. 2023). It has also been utilized in GNN to improve the performance (Wang et al. 2023; Han et al. 2024), diversify node representations in fairness-augmented graphs (Liu et al. 2023b), and deal with class imbalance (Hu et al. 2021). Previous work (Shazeer et al. 2017) has employed hierarchical expert routing to improve memory efficiency, enabling a larger number of experts. However, previous papers have not shown the performance gain of hierarchical MoEs than regular MoEs when using the same number of total experts.

Preliminary

Task Definition

HLS prediction is formalized as a graph regression task. Following previous works (Sohrabizadeh et al. 2022, 2023), we utilize ProGraML (Cummins et al. 2021) graph to represent a source code, which is a control data flow graph. Nodes represent instructions, variables, and constant values, and edges represent the control flow and data flow. A GNN model is trained to predict the FPGA’s latency and the utilization of four resources: LUT, FF, DSP, and BRAM. In the domain generalization setting, we train the model on N source kernels $D^{(train)} = \{D_1, D_2, \dots, D_N\}$, where $D_i = \{(X_i, T_{i1}, Y_{i1}), (X_i, T_{i2}, Y_{i2}), \dots, (X_i, T_{ii_n}, Y_{ii_n})\}$ is the i -th kernel containing i_n samples, and each sample consists of a program X , a pragma design T , and a label Y .

For a new kernel D_{test} , we mimic the data-scarce situation where we only use k samples from the dataset $D^{(k)} \subset D_{test}, |D^{(k)}| = k$, to fine-tune the model. After fine-tuning, there are two ways of evaluation: offline evaluation and online evaluation. In the offline evaluation, we evaluate the MSE on the left-out test samples: $D_{test} \setminus D^{(k)}$. In the online evaluation, we run a DFS searching algorithm used by previous works (Sohrabizadeh et al. 2022, 2023) to search for good pragma designs. Based on the fine-tuned model’s prediction, We select the top-10 pragma designs, run HLS for them, and evaluate the FPGA’s speedup compared to AutoDSE.

HARP Model

The proposed hierarchical MoE can be adapted to any GNN model. We use one of the SOTA GNN models for HLS prediction, HARP (Sohrabizadeh et al. 2023), as the base model. Since the original ProGraML graph is sparse and not good at modeling long-term dependency, HARP creates a “pseudo node” for each basic block in the program and connects it with every node within that basic block. Defined by the compiler community, a basic block is a sequence of instructions that has a single entry point and a single exit point, whose terminator instruction can be branch, return, etc. We illustrate HARP’s model structure in the appendix. We use V to denote the set of all nodes and V_B to denote the set of pseudo nodes. HARP consists of five components: (1) GNN encoder: it consists of 6 GNN layers and learns node representation; (2) Pragma MLP: it uses an MLP for each pragma type to transform the representation of pseudo nodes that are modified by that pragma type; (3) Another GNN layer after pragma MLP: it spreads the information of pragmas from pseudo nodes to normal nodes and to pseudo nodes that do not have pragmas; (4) Graph pooling: it does graph pooling on pseudo nodes V_B to form a graph representation and on normal nodes $V \setminus V_B$ to form another graph representation, then it concatenates them; (5) Output MLP: it makes the prediction based on the graph representation.

Methods

Low-Level Mixture of Experts

A unique opportunity for our task is that the input graph has three granularities: normal nodes that represent data and instructions, pseudo nodes that represent basic blocks, and the whole graph that represents a source code file. If a data point from the target kernel shares a similar statement (node), basic block, or even the whole code (graph) with a data point from the training kernels, MoE could be helpful. Thus, we consider employing MoE on the three granularities: MoE on all nodes including normal nodes and pseudo node (node MoE), MoE only on pseudo nodes (block MoE), and MoE on the graph (graph MoE). Based on our pre-exploration, the best practice is to apply MoE in the components after the pragma MLP, since the experts need to share the same encoder and pragma MLPs. Our design of the three low-level MoE models is illustrated in Figure 2.

Node MoE. For the MoE that operates on all nodes, we apply it on the GNN layer after the pragma MLP. We train

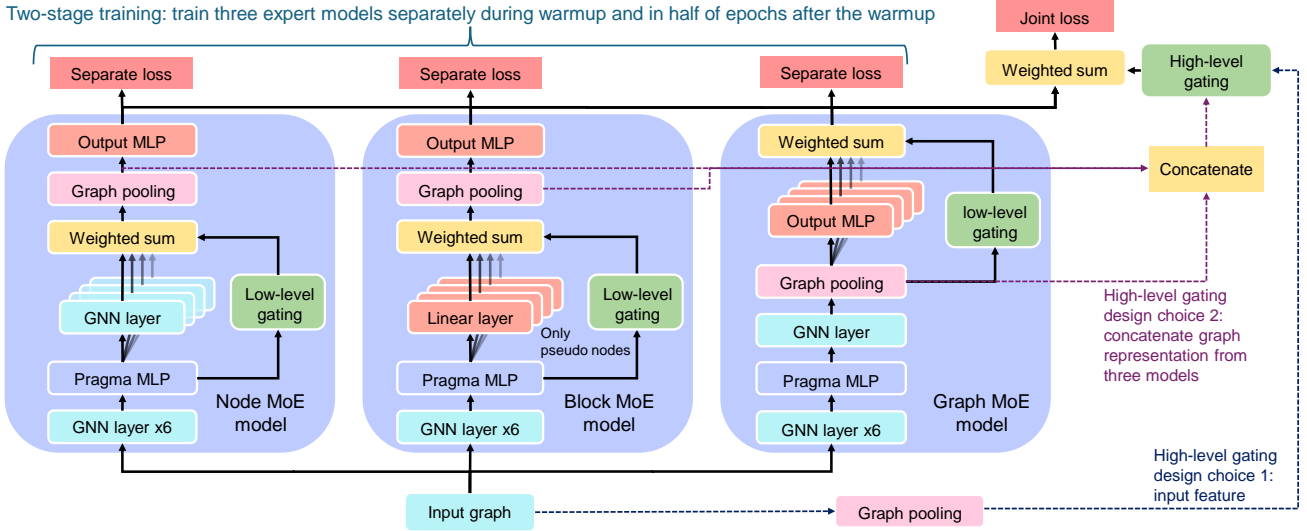


Figure 2: Illustration of hierarchical MoE. The three low-level models are aggregated via the high-level gating network.

n GNN layers of the same structure as n experts. We denote the representation of node v_i after the pragma MLP as $\mathbf{h}_i \in \mathbb{R}^d$. The node MoE is formulated as:

$$\mathbf{h}'_i = \sum_{j=1}^n \text{softmax}(\mathbf{W}_G \mathbf{h}_i)_j \cdot \text{GNN}_j(\mathbf{h}_i, \text{Graph}), \quad (1)$$

where $\mathbf{W}_G \in \mathbb{R}^{n \times d}$ is the parameter of the gating network, and $\text{GNN}_j(\cdot)$ is the j -th expert. The softmax function ensures that all experts' weights sum up to 1. By employing the MoE layer, different nodes can utilize different parameters for message passing and message aggregation.

Block MoE. We have tried applying MoE on the pragma MLP, but the performance has decreased. It might be because each pragma type has a separate pragma MLP, so the training data for each pragma MLP is already not abundant. If we further apply MoE, it will dilute the training data even more and hinder the performance. Instead, we add an additional MoE layer on the pseudo nodes' representations after the pragma MLP, so that we can increase the expressiveness of the pseudo nodes' representations before graph pooling. The representation space of the pseudo nodes after the block MoE could be different from normal nodes, so it is no longer suitable to have another GNN layer after the pragma MLP to do message passing between pseudo nodes and normal nodes. We have also tried applying an additional layer for normal nodes after the pragma MLP, but the performance is unsatisfactory. It might be because the normal nodes lack a global view, so it is not useful to further transform its representation by another layer. After having the block MoE, doing graph pooling only on the pseudo nodes performs better than doing graph pooling on both pseudo nodes and normal nodes. Therefore, we do not utilize normal nodes after the GNN encoder in the block MoE model.

We use n linear layers as n expert networks. We denote the representation of pseudo node v_i after the pragma MLP as $\mathbf{h}_i \in \mathbb{R}^d$. The block MoE is formulated as:

$$\mathbf{h}'_i = \sum_{j=1}^n \text{softmax}(\mathbf{W}_G \mathbf{h}_i)_j \cdot \mathbf{W}_{e_j} \mathbf{h}_i \quad (v_i \in V_B), \quad (2)$$

where $\mathbf{W}_G \in \mathbb{R}^{n \times d}$ is the parameter of the gating network, and $\mathbf{W}_{e_j} \in \mathbb{R}^{d \times d}$ is the j -th expert network.

Graph MoE. We apply the graph MoE on the output MLP. We denote the graph representation after graph pooling as \mathbf{h}_G . Different from the block MoE structure, here we use the original pragma MLP and graph pooling structures as HARP. We employ the output MLP as the expert network. The graph MoE is formulated as:

$$\hat{Y}^{(t)} = \sum_{j=1}^n \text{softmax}(\mathbf{W}_G \mathbf{h}_G)_j \cdot \text{MLP}^{(t)}_j(\mathbf{h}_G), \quad (3)$$

where $\text{MLP}^{(t)}_j(\cdot)$ is the j -th expert MLP for predicting the target t (the target could be the FPGA's latency or a certain resource's utilization). It contains four linear layers and the ELU activation function between them. The graph MoE enables different design points to utilize different parameters to make the final prediction.

Regularization term. As discovered in many literature (Shazeer et al. 2017; Wang et al. 2023; Li et al. 2023), expert polarization is a common problem of MoE. Due to the random initialization of expert networks, different experts initially have different performances, and the gating network learns to assign higher weights to better experts. It results in more training of better experts, leading to their better performance, which in turn leads to their higher weights. As training continues, the MoE model might collapse and only use the best expert. To encourage balanced expert assignments, we apply a regularization term (Shazeer et al. 2017):

$$L_R = CV(\mathbf{I}(\mathbf{W}_G)), \quad \mathbf{I}(\mathbf{W}_G) = \sum_{i=1}^M \text{softmax}(\mathbf{W}_G \mathbf{h}_i), \quad (4)$$

where $CV(\cdot)$ is the coefficient of variation. We calculate the importance score $I(W_G) \in \mathbb{R}^n$ for gating network W_G as the total weights assigned to each expert. For node MoE, M is the total number of nodes in all graphs; for block MoE, M is the total number of pseudo nodes in all graphs; for graph MoE, M is the number of graphs.

High-Level Mixture of Experts

Now we have three MoE models operating on different granularities. A simple approach to combining them is to use all of them together in one model. However, our ablation study verifies that the performance will be worse. This demonstrates that we only need MoE on one granularity in one model. However, the best granularity greatly varies for different kernels, and it is difficult to discover a pattern. Therefore, we propose a high-level MoE to aggregate them. It calculates the weighted sum of the outputs of the three low-level MoE models.

We propose two designs of the high-level gating network, as illustrated in Figure 2. The first design is to do graph pooling on the input node features to form a graph representation as the input to the high-level gating network. We use the self-attention graph pooling. Denoting the input feature of node v_i as x_i , the graph pooling is formalized as:

$$x_G = \sum_{i \in V} \text{softmax}(MLP(x_i)) \cdot x_i \quad (5)$$

where X_G is the aggregated input feature, and V is the set of all nodes. The second design is to concatenate the graph representation in the three low-level MoE models. The second design performs better in our experiments, since the hidden representations are more expressive than the input features. Nonetheless, when we use a sparse MoE where only one or two experts are selected, the first design will be more memory efficient. It can determine the expert assignment before the computation of three expert models, thus reducing unnecessary computation. However, the best-performing method is to utilize all the experts, and in this case, the two designs are similar in efficiency. We utilize all the experts in our experiments. We also apply the regularization term for the high-level gating network.

Two-Stage Training and Constant Initialization

Optimizing the hierarchical MoE is challenging. Different from previous MoE studies where expert networks have the same or similar structures, our three low-level MoEs are very different and thus have different convergence speeds. The graph MoE model converges the fastest, since its MoE operates on the graph representation and has the least computation. Thus, the high-level gating network suffers severely from expert polarization, leaning towards the graph MoE model. If we simply increase the weight of the regularization term, the high-level gating network can effectively learn to assign about $\frac{1}{3}$ weight to each expert, but the graph MoE model still converges much faster than the other two models. In the first few epochs, the output of node MoE and block MoE models will be noisy and thus they are discouraged

from making predictions. As a result, the graph MoE model will learn to output three times the label, while node and block MoE models will learn to output zero.

To address this unique challenge, we design a two-stage training strategy to encourage every expert model to perform well individually. In the first stage containing T epochs (warmup), we train the three expert models individually. In the second stage, we take turns training the whole model end-to-end and the three expert models individually. If we denote the label as Y , the prediction made by the i -th expert model as \hat{Y}_i , and the MSE loss function as $L(Y, \hat{Y}_i)$, then we define the loss function at epoch t as:

$$L = \begin{cases} L(Y, \hat{Y}_1) + L(Y, \hat{Y}_2) + L(Y, \hat{Y}_3) + \alpha L_R, & \text{if } t < T \text{ or } 2 \mid t. \\ L(Y, \sum_{i=1}^3 g_i \cdot \hat{Y}_i) + \alpha L_R + \beta L_{Rh}, & \text{otherwise.} \end{cases} \quad (6)$$

Here, $L_R = \frac{1}{3}(L_{R1} + L_{R2} + L_{R3})$, where L_{Ri} is the regularization term of the i -th low-level MoE. L_{Rh} is the regularization term of the high-level MoE. g_i is the weight assigned by the high-level gating network. When we fine-tune our model on target kernels, we directly use the end-to-end joint training, since all the experts can already perform well during fine-tuning and there is no risk of expert polarization.

In common situations where the expert networks have similar or the same structures, the gating network’s parameters should be randomly initialized, because we need the randomness to diversify the experts. Instead, we initialize the high-level gating network to assign the same weights to the expert models, which can further prevent expert polarization. For low-level MoEs, we use random initialization.

Experiments

Experiment Settings

Datasets. We use the most comprehensive benchmark dataset, HLSyn (Bai et al. 2023). It consists of 42 kernels covering various categories: linear algebra on vectors and matrices, data mining, stencil operations, etc. We utilize the AMD/Xilinx HLS tool, Vitis 2021.1 (AMD/Xilinx 2020), to run HLS targeting the Xilinx Alveo U200 FPGA with a working frequency of 250MHz. We select 6 kernels as the target kernels that span representative categories including linear algebra computation, data mining, and stencil computation, and we use the other kernels as source kernels. Table 2 shows the dataset statistics. We introduce the kernels’ details in the appendix. The HLSyn dataset was generated by running the bottleneck-based heuristics method, AutoDSE (Sohrabzadeh et al. 2021), for 24 hours. Many designs explored by AutoDSE are unavailable in HLS, so we collect this information to train a HARP classification model. Since its accuracy already exceeds 95%, there is no need to employ MoE on the classification model. We use the available designs in the dataset to train the regression model, and we employ MoE on the regression model.

Models. Based on our pre-exploration, we use 4 experts in the low-level MoEs, and we set the weight of the regularization term of both low-level and high-level MoE, α and

Table 1: Domain generalization performance. “Geo mean” is the geometric mean speedup.

MoE category	Model	Offline evaluation	Online evaluation (FPGA speedup compared to AutoDSE)							
		Total MSE	Fd	Gemv	Sy	Gemm	Ja	Tr	Average	Geo mean
No MoE	HARP	0.202±0.013	1.03	1.29	1	1	1.08	1.18	1.10	1.09
	HARP+MAML	0.732±0.167	1	1	1	1	1	1	1	1
	ProgSG	0.486±0.059	1	1	1	1	1	1.22	1.04	1.03
Single MoE	Node MoE	0.160±0.035	1.13	1.03	1.00	1	1	1.15	1.05	1.05
	Block MoE	0.171±0.019	1.43	1.11	1	1	1	1.07	1.10	1.09
	Graph MoE	0.216±0.046	1	1.28	1.01	1	1.08	1.33	1.12	1.11
Hierarchical MoE		0.143±0.028	3.85	1.46	1	1.01	1	1.23	1.59	1.38

Table 2: Dataset Statistics. “#Class” and “#Regre” denote the number of classification and regression data. The kernel acronyms represent “fdtd-2d-large”, “gemver-medium”, “syr2k”, “gemm-p”, “jacobi-2d”, and “trmm-opt”.

	Source	Fd	Gemv	Sy	Gemm	Ja	Tr
#Class	36185	418	428	526	1421	1837	1651
#Regre	9086	77	231	121	348	257	103

β , to $5e-3$. Our baselines include the SOTA GNN method, HARP (Sohrabizadeh et al. 2023); HARP+MAML (Bai et al. 2022), which applies the meta-learning method MAML (Finn, Abbeel, and Levine 2017) on this task proposed by (Bai et al. 2022), since MAML could learn a more generalizable initialization of parameters; and ProgSG (Qin et al. 2024), which combines HARP and language model.

Evaluation. We train the regression and classification models on the source kernels. We want to mimic the domain transfer situation of having scarce but representative labeled data on the target kernels, so we use 50 data points per kernel to fine-tune our regression model, and roughly the same ratio of data points, 265 samples per kernel, to fine-tune the classification model. To select representative data points, we use K-means based on the graph representation. As introduced in the preliminary, we conduct both offline and online evaluations. In offline evaluation, we calculate the fine-tuned model’s mean squared error (MSE) on the left-out data points in the target kernels. In the online evaluation, we use the DFS search used in previous studies (Sohrabizadeh et al. 2022, 2023) to search for pragma designs. We limit our search range to 75,000 pragma designs and the time of an hour, since it typically takes about an hour to traverse 75,000 designs. We use the fine-tuned classification model to predict the validity and the fine-tuned regression model to predict the FPGA’s latency and resource utilization. From designs that are predicted to be valid and satisfy resource constraints, we choose the top 10 designs with the lowest predicted latencies. We run HLS for them and pick up the best valid design that has the lowest latency. Since we have used the dataset to fine-tune, we pick the best design from the selected top-10 designs and the dataset, and calculate its speedup compared to the best design in the dataset. We run the offline evaluation five times and the online evaluation three times, then report the mean results.

Experiment Results

Table 1 shows the main results. In the main experiments, we use the second design of the high-level gating network as it performs better. Neither MAML nor ProgSG performs well in our setting. It might be because we have many more source kernels compared to the previous paper that utilizes MAML on this task (Bai et al. 2022). Different kernels might result in different directions of the meta gradient, leading to unstable meta-learning. ProgSG which combines GNN and language models has a strong ability on the HLSyn dataset when the training data is sufficient (Qin et al. 2024), but since the language model needs a large dataset to fine-tune, it severely overfits in our data-scarce setting. During fine-tuning, the training loss is lower than 0.05, but the test loss is high. Comparatively, the hierarchical MoE is a more generalizable structure. In the online evaluation, on most kernels, the best of three single MoE models outperforms HARP, but different kernels favor different low-level MoEs. For example, the block MoE model performs better than the node MoE and the graph MoE for “Fd”, while graph MoE is the best for “Gemv”, “Ja”, and “Tr”. Since a single MoE model could not perform well on all kernels, its overall MSE and the average speedup might not outperform HARP. By aggregating them together, the hierarchical MoE performs the best or close to the best on almost every kernel. Its geometric mean speedup achieves about 26.6% higher than HARP.

Table 3: Using MoE on various granularities in a single model. “N”, “B”, and “G” represent node, block, and graph. Apart from selecting 50 representative points by K-means for fine-tuning, we also experiment with random data split. The hierarchical MoE model shows the highest stability when the data quality is worse due to random split.

Data split	N+B	N+G	B+G	N+B+G	Hierarchy
K-means	0.341	0.213	0.188	0.174	0.143
Random	0.893	0.562	3.126	0.984	0.452

Various model structures. To verify the effectiveness of our elaborate model design, we run extensive experiments on various model structures. First, instead of aggregating the three low-level MoEs, can we apply MoE on the three granularities together in a single model? We specify the detailed structure design in the appendix. Table 3 shows the results.

When we use MoE on two or three granularities in a single model, the loss is usually higher than the lowest loss when using only one granularity. Apart from selecting 50 representative data points by K-means for fine-tuning, we also experiment with random data split. We use the same random split for all models to ensure fair comparison. Hierarchical MoE is the most stable model when it faces low-quality fine-tuning data in the random split. If we stack MoE on various granularities in the same model, the structure might be too complex and thus unstable to train on a small dataset.

Table 4: Using MoE on a single granularity in the hierarchical MoE. “Node/Block/Graph” means only using MoE on the node/block/graph granularity in the hierarchical MoE. “All” means aggregating the three granularities.

Metric	Node	Block	Graph	All
Offline (MSE)	0.164	0.177	0.279	0.143
Online (geo mean speedup)	1.34	1.13	1.35	1.38

Second, does the hierarchical MoE benefit from combining the three granularities? To answer it, we still use the hierarchical MoE structure, but we use the same low-level MoE model as the three experts of the high-level MoE. Table 4 shows the results. It verifies that aggregating the three granularities performs the best. Using only the node MoE or graph MoE also performs well in the online evaluation, and this might be due to the increased number of experts. Nonetheless, aggregating the three granularities could further improve the performance. Third, to verify whether the performance gain simply comes from having more parameters, we enlarge the hidden size of the HARP model from 64 to 128 or 256, and the model loss increases. Due to the space limit, the results are in the appendix. Therefore, the key is the MoE structure instead of a larger parameter size.

Table 5: Ablation study of two-stage training and high-level gating network. “Input” means that the high-level gating network utilizes the input features, and “Hidden” means that it utilizes the hidden representations.

Gating	Two-stage training		W/o alternative train		W/o warmup	
	Input	Hidden	Input	Hidden	Input	Hidden
MSE	0.149	0.143	0.193	0.159	0.152	0.184

Fourth, we conduct an ablation study on the two-stage training and the high-level gating network’s design, and the results are listed in Table 5. There are two components in the two-stage training: the warmup epochs, and training three experts jointly and separately in turn after the warmup. We either disable the alternative training or the warmup. The lowest MSE is achieved when we use both of them. Also, the high-level gating network based on hidden representations is better than that based on input features.

Analysis of Expert Assignment

We want to unveil the mystery of the gating networks. We show the average assigned weights by the high-level gating

Table 6: Average assigned weights of the high-level MoE.

Expert	Fd	Gemv	Sy	Gemm	Ja	Tr
Node MoE	37%	29%	36%	37%	46%	27%
Block MoE	49%	28%	26%	40%	32%	37%
Graph MoE	14%	43%	38%	23%	22%	36%

network in Table 6. According to Table 1, “Fd”, “Gemv” and “Tr” have a strong preference for a certain granularity, while the other three kernels do not. Among them, the block MoE performs the best for “Fd”, and it is also assigned the highest weight; graph MoE is the best expert for “Gemv” and “Tr”, and it is also assigned the highest or nearly the highest weight. The weights are partially explainable.

Table 7: Average assigned weights of the block MoE. Each column shows the expert weights for pseudo nodes modified by a certain type of pragma. “0<parallel≤4” and “parallel>4” indicate the range of the parallelization factor.

Expert	No pragma	Loop tiling	Pipeline	0<Parallel≤4	Parallel>4
1	32%	6%	6%	4%	2%
2	18%	8%	13%	41%	81%
3	22%	64%	60%	43%	8%
4	28%	22%	21%	12%	10%

We pick the best hierarchical MoE model based on the previous five repeated offline evaluation experiments to do a case study on the low-level MoE. Due to the limited space, here we only analyze the block MoE, and we analyze the node and graph MoEs in the appendix. The pragmas modify the pseudo nodes but not normal nodes, so block MoE is a window for us to analyze the pragmas. We summarize the weights of each expert for each pragma type in Table 7. There are three types of pragmas: loop tiling, pipeline, and parallelization. The third expert is good at dealing with loop tiling, pipeline, and small parallel factors; the second expert is good at dealing with large parallel factors; the other two experts deal more with pseudo nodes that do not have pragmas. Different experts diversify their roles, which improves domain generalizability.

Conclusion

Domain generalization is a big challenge for HLS prediction models. Based on the unique challenges and opportunities of this task, we propose the hierarchical MoE structure, where different expert networks can specialize in different regions, and it can be flexibly adapted to any GNN model. In the low-level MoE, we apply MoE on the three natural granularities of the graph: nodes, basic blocks, and the graph. In the high-level MoE, we aggregate the three low-level MoE models, so that different data points can flexibly decide which granularity to utilize MoE. To address the severe expert polarization, we propose two-stage training via deactivating the high-level gating network for some epochs. Extensive experiments have verified the effectiveness of hierarchical MoE. We focus on the generalizability of the HLS prediction task, but our model might also potentially improve the generalizability in other applications of various domains.

Acknowledgments

This work was partially supported by NSF grants 2211557, 1937599, 2119643, and 2303037, SRC JUMP 2.0 PRISM Center, NASA, Okawa Foundation, Amazon Research, Cisco, Picsart, Snapchat, and the CDSC industrial partners (<https://cdsc.ucla.edu/partners/>). The authors would also like to thank AMD/Xilinx for HACC equipment donation, and Marci Baun for editing the paper. J. Cong has a financial interest in AMD.

References

- AMD/Xilinx. 2020. Vitis HLS. <https://docs.xilinx.com/v/u/2020.2-English/ug1416-vitis-documentation>.
- Bai, Y.; Sohrabizadeh, A.; Qin, Z.; Hu, Z.; Sun, Y.; and Cong, J. 2023. Towards a Comprehensive Benchmark for High-Level Synthesis Targeted to FPGAs. *Advances in Neural Information Processing Systems*, 36: 45288–45299.
- Bai, Y.; Sohrabizadeh, A.; Sun, Y.; and Cong, J. 2022. Improving GNN-based accelerator design automation with meta learning. In *Proceedings of the 59th ACM/IEEE Design Automation Conference, DAC '22*, 1347–1350. Association for Computing Machinery. ISBN 9781450391429.
- Cong, J.; Lau, J.; Liu, G.; Neuendorffer, S.; Pan, P.; Vissers, K.; and Zhang, Z. 2022. FPGA HLS today: successes, challenges, and opportunities. *ACM Transactions on Reconfigurable Technology and Systems (TRETS)*, 15(4): 1–42.
- Cong, J.; Liu, B.; Neuendorffer, S.; Noguera, J.; Vissers, K.; and Zhang, Z. 2011. High-Level Synthesis for FPGAs: From Prototyping to Deployment. *IEEE Transactions on Computer-Aided Design of Integrated Circuits and Systems*, 30(4): 473–491.
- Cummins, C.; Fisches, Z. V.; Ben-Nun, T.; Hoefler, T.; O’Boyle, M. F.; and Leather, H. 2021. ProGraML: A graph-based program representation for data flow analysis and compiler optimizations. In *International Conference on Machine Learning*, 2244–2253. PMLR.
- Dai, Q.; Shen, X.; Wu, X.; and Wang, D. 2019. Network Transfer Learning via Adversarial Domain Adaptation with Graph Convolution. *CoRR*, abs/1909.01541.
- Finn, C.; Abbeel, P.; and Levine, S. 2017. Model-Agnostic Meta-Learning for Fast Adaptation of Deep Networks. arXiv:1703.03400.
- Han, H.; Li, J.; Huang, W.; Tang, X.; Lu, H.; Luo, C.; Liu, H.; and Tang, J. 2024. Node-wise Filtering in Graph Neural Networks: A Mixture of Experts Approach. *arXiv preprint arXiv:2406.03464*.
- Hu, F.; Wang, L.; Wu, S.; Wang, L.; and Tan, T. 2021. Graph classification by mixture of diverse experts. *arXiv preprint arXiv:2103.15622*.
- Jacobs, R.; Jordan, M.; Nowlan, S.; and Hinton, G. 1991. Adaptive Mixture of Local Expert. *Neural Computation*, 3: 78–88.
- Kwon, J.; and Carloni, L. P. 2020. Transfer Learning for Design-Space Exploration with High-Level Synthesis. In *2020 ACM/IEEE 2nd Workshop on Machine Learning for CAD (MLCAD)*, 163–168.
- Li, B.; Shen, Y.; Yang, J.; Wang, Y.; Ren, J.; Che, T.; Zhang, J.; and Liu, Z. 2023. Sparse Mixture-of-Experts are Domain Generalizable Learners. arXiv:2206.04046.
- Liu, Y.; Ao, X.; Feng, F.; Ma, Y.; Li, K.; Chua, T.-S.; and He, Q. 2023a. FLOOD: A flexible invariant learning framework for out-of-distribution generalization on graphs. In *Proceedings of the 29th ACM SIGKDD Conference on Knowledge Discovery and Data Mining*, 1548–1558.
- Liu, Z.; Zhang, C.; Tian, Y.; Zhang, E.; Huang, C.; Ye, Y.; and Zhang, C. 2023b. Fair graph representation learning via diverse mixture-of-experts. In *Proceedings of the ACM Web Conference 2023*, 28–38.
- Loshchilov, I.; and Hutter, F. 2017. SGDR: Stochastic Gradient Descent with Warm Restarts. arXiv:1608.03983.
- Ma, J.; and Yarats, D. 2021. On the adequacy of untuned warmup for adaptive optimization. arXiv:1910.04209.
- Pouchet, L.-N. 2012. PolyBench/C. <https://web.cs.ucla.edu/~pouchet/software/polybench/>.
- Pouget, S.; Pouchet, L.-N.; and Cong, J. 2024a. Automatic Hardware Pragma Insertion in High-Level Synthesis: A Non-Linear Programming Approach. arXiv:2405.12304.
- Pouget, S.; Pouchet, L.-N.; and Cong, J. 2024b. Enhancing High-Level Synthesis with Automated Pragma Insertion and Code Transformation Framework. arXiv:2405.03058.
- Qin, Z.; Bai, Y.; Sohrabizadeh, A.; Ding, Z.; Hu, Z.; Sun, Y.; and Cong, J. 2024. Cross-Modality Program Representation Learning for Electronic Design Automation with High-Level Synthesis. arXiv:2406.09606.
- Reagen, B.; Adolf, R.; Shao, Y.; Wei, G.-Y.; and Brooks, D. 2014. MachSuite: Benchmarks for accelerator design and customized architectures. 110–119.
- Schafer, B. C.; and Wang, Z. 2019. High-level synthesis design space exploration: Past, present, and future. *IEEE Transactions on Computer-Aided Design of Integrated Circuits and Systems*, 39(10): 2628–2639.
- Shazeer, N.; Mirhoseini, A.; Maziarz, K.; Davis, A.; Le, Q. V.; Hinton, G. E.; and Dean, J. 2017. Outrageously Large Neural Networks: The Sparsely-Gated Mixture-of-Experts Layer. *CoRR*, abs/1701.06538.
- Shen, X.; Pan, S.; Choi, K.-S.; and Zhou, X. 2023. Domain-adaptive message passing graph neural network. *Neural Networks*, 164: 439–454.
- Sohrabizadeh, A.; Bai, Y.; Sun, Y.; and Cong, J. 2022. Automated Accelerator Optimization Aided by Graph Neural Networks. In *2022 59th ACM/IEEE Design Automation Conference (DAC)*.
- Sohrabizadeh, A.; Bai, Y.; Sun, Y.; and Cong, J. 2023. Robust GNN-based representation learning for HLS. In *2023 IEEE/ACM International Conference on Computer Aided Design (ICCAD)*, 1–9. IEEE.
- Sohrabizadeh, A.; Yu, C. H.; Gao, M.; and Cong, J. 2021. AutoDSE: Enabling Software Programmers to Design Efficient FPGA Accelerators. arXiv:2009.14381.
- Ustun, E.; Deng, C.; Pal, D.; Li, Z.; and Zhang, Z. 2020. Accurate operation delay prediction for FPGA HLS using

graph neural networks. In *Proceedings of the 39th international conference on computer-aided design*, 1–9.

Wang, H.; Jiang, Z.; You, Y.; Han, Y.; Liu, G.; Srinivasa, J.; Kompella, R. R.; and Wang, Z. 2023. Graph Mixture of Experts: Learning on Large-Scale Graphs with Explicit Diversity Modeling. arXiv:2304.02806.

Wu, M.; Pan, S.; Zhou, C.; Chang, X.; and Zhu, X. 2020. Unsupervised Domain Adaptive Graph Convolutional Networks.

Wu, N.; Xie, Y.; and Hao, C. 2021. Ironman: GNN-assisted Design Space Exploration in High-Level Synthesis via Reinforcement Learning. In *Proceedings of the 2021 on Great Lakes Symposium on VLSI*, 39–44. IEEE.

Wu, N.; Xie, Y.; and Hao, C. 2023. IronMan-Pro: Multi-objective Design Space Exploration in HLS via Reinforcement Learning and Graph Neural Network-Based Modeling. *IEEE Transactions on Computer-Aided Design of Integrated Circuits and Systems*, 42(3): 900–913.

Wu, N.; Yang, H.; Xie, Y.; Li, P.; and Hao, C. 2022a. High-level synthesis performance prediction using GNNs: benchmarking, modeling, and advancing. In *Proceedings of the 59th ACM/IEEE Design Automation Conference, DAC '22*, 49–54. New York, NY, USA: Association for Computing Machinery. ISBN 9781450391429.

Wu, Q.; Zhang, H.; Yan, J.; and Wipf, D. 2022b. Handling Distribution Shifts on Graphs: An Invariance Perspective. In *International Conference on Learning Representations (ICLR)*.

Wu, S.; Cao, K.; Ribeiro, B.; Zou, J.; and Leskovec, J. 2024. GraphMETRO: Mitigating Complex Graph Distribution Shifts via Mixture of Aligned Experts. arXiv:2312.04693.

Zhang, Y.; Song, G.; Du, L.; Yang, S.; and Jin, Y. 2019. DANE: Domain Adaptive Network Embedding. In *Proceedings of the Twenty-Eighth International Joint Conference on Artificial Intelligence, IJCAI-19*, 4362–4368. International Joint Conferences on Artificial Intelligence Organization.

Zhong, T.; Chi, Z.; Gu, L.; Wang, Y.; Yu, Y.; and Tang, J. 2023. Meta-DMoE: Adapting to Domain Shift by Meta-Distillation from Mixture-of-Experts. arXiv:2210.03885.

Reproducibility Checklist

This paper:

- Includes a conceptual outline and/or pseudocode description of AI methods introduced. (yes/partial/no/NA) Yes.
- Clearly delineates statements that are opinions, hypotheses, and speculations from objective facts and results. (yes/no) Yes.
- Provides well-marked pedagogical references for less-familiar readers to gain the background necessary to replicate the paper. (yes/no) Yes.

Does this paper make theoretical contributions? (yes/no) No. If yes, please complete the list below.

- All assumptions and restrictions are stated clearly and formally. (yes/partial/no)

- All novel claims are stated formally (e.g., in theorem statements). (yes/partial/no)
- Proofs of all novel claims are included. (yes/partial/no)
- Proof sketches or intuitions are given for complex and/or novel results. (yes/partial/no)
- Appropriate citations to theoretical tools used are given. (yes/partial/no)
- All theoretical claims are demonstrated empirically to hold. (yes/partial/no/NA)
- All experimental codes used to eliminate or disprove claims are included. (yes/no/NA)

Does this paper rely on one or more datasets? (yes/no) Yes. If yes, please complete the list below.

- A motivation is given for why the experiments are conducted on the selected datasets. (yes/partial/no/NA) Yes.
- All novel datasets introduced in this paper are included in a data appendix. (yes/partial/no/NA) NA (We only used existing public benchmark datasets).
- All novel datasets introduced in this paper will be made publicly available upon publication of the paper with a license that allows free usage for research purposes. (yes/partial/no/NA) NA (We only used existing public benchmark datasets).
- All datasets drawn from the existing literature (potentially including authors' own previously published work) are accompanied by appropriate citations. (yes/no/NA) Yes.
- All datasets drawn from the existing literature (potentially including authors' own previously published work) are publicly available. (yes/partial/no/NA) Yes.
- All datasets that are not publicly available are described in detail, with explanation why publicly available alternatives are not scientifically satisfying. (yes/partial/no/NA) NA (We only used public benchmark datasets).

Does this paper include computational experiments? (yes/no) Yes. If yes, please complete the list below.

- Any code required for pre-processing data is included in the appendix. (yes/partial/no) Yes.
- All source code required for conducting and analyzing the experiments is included in a code appendix. (yes/partial/no) Yes.
- All source code required for conducting and analyzing the experiments will be made publicly available upon publication of the paper with a license that allows free usage for research purposes. (yes/partial/no) Yes.
- All source code implementing new methods have comments detailing the implementation, with references to the paper where each step comes from. (yes/partial/no) Yes.
- If an algorithm depends on randomness, then the method used for setting seeds is described in a way sufficient to allow replication of results. (yes/partial/no/NA) Yes.

- This paper specifies the computing infrastructure used for running experiments (hardware and software), including GPU/CPU models; amount of memory; operating system; names, and versions of relevant software libraries and frameworks. (yes/partial/no) Yes.
- This paper formally describes evaluation metrics used and explains the motivation for choosing these metrics. (yes/partial/no) Yes.
- This paper states the number of algorithm runs used to compute each reported result. (yes/no) Yes.
- Analysis of experiments goes beyond single-dimensional summaries of performance (e.g., average; median) to include measures of variation, confidence, or other distributional information. (yes/no) Yes.
- The significance of any improvement or decrease in performance is judged using appropriate statistical tests (e.g., Wilcoxon signed-rank). (yes/partial/no) Partial (We run the offline evaluation experiments five times and online evaluation experiments three times, and we report the mean performance and the standard deviation).
- This paper lists all final (hyper-)parameters used for each model/algorithm in the paper's experiments. (yes/partial/no/NA) Yes (The most important hyper-parameters are listed in the appendix. Others are in the codes that we submit).
- This paper states the number and range of values tried per (hyper-) parameter during the development of the paper, along with the criterion used for selecting the final parameter setting. (yes/partial/no/NA) Yes.

Additional Background Knowledge of HLS

As the HLS prediction task is quite new to the AI community, we would like to illustrate this task at the beginning of the appendix. Taking the “syr2k” kernel as an example, Figure 3 shows its source code. As explained in the Introduction section, the source code consists of the program that describes the FPGA’s function, which is similar to any normal C program, and several pragmas. Now the pragmas are represented by the placeholders “auto{pragma index}”. We utilize the machine learning model to find the best pragmas to insert in these placeholders.

```
#pragma ACCEL kernel

void kernel_syr2k(double alpha, double beta, double C[80][80], double
A[80][60], double B[80][60])
{
    int i;
    int j;
    int k;

#pragma ACCEL PIPELINE auto{__PIPE__L0}

#pragma ACCEL TILE FACTOR=auto{__TILE__L0}

#pragma ACCEL PARALLEL FACTOR=auto{__PARA__L0}
    for (i = 0; i < 80; i++) {

#pragma ACCEL PARALLEL FACTOR=auto{__PARA__L1}
        for (j = 0; j < 80; j++) {
            if (j <= i) {
                C[i][j] *= beta;
            }
        }
    }

#pragma ACCEL PIPELINE auto{__PIPE__L2}

#pragma ACCEL TILE FACTOR=auto{__TILE__L2}

#pragma ACCEL PARALLEL FACTOR=auto{__PARA__L2}
    for (k = 0; k < 60; k++) {

#pragma ACCEL PARALLEL FACTOR=auto{__PARA__L3}
        for (j = 0; j < 80; j++) {
            if (j <= i) {
                C[i][j] += A[j][k] * alpha * B[i][k] + B[j][k] * alpha * A[i][k];
            }
        }
    }
}
}
```

Figure 3: Source code of the “syr2k” kernel. The source code consists of the program that describes the FPGA’s function, and several pragmas inserted in the program that instruct the hardware synthesis process, such as parallelization, pipeline, etc. “auto{pragma index}” are pragma’s placeholders. We utilize the machine learning model to find the best pragmas to insert in these placeholders.

Table 8: Introduction of pragmas.

Pragma type	Option	Meaning
Parallel	An integer	Number of loop iterations to parallelize
Pipeline	”Off”	No pipeline
	”Flatten” NA	Fine-grained pipeline Coarse-grained pipeline
Loop tiling	An integer	The factor of loop tiling

There are three types of pragmas: parallel, pipeline, and loop tiling. For the parallel pragma placeholders, we should insert an integer as the parallel factor. For the pipeline

pragma placeholders, we should choose between the fine-grained pipeline, coarse-grained pipeline, or not using the pipeline. For the loop tiling pragma placeholders, we should insert an integer as the loop tiling factor. Table 8 lists the introduction of the pragmas.

Designing the pragmas is labor-intensive and heavily relies on hardware knowledge, which motivates the automated pragma design research. Different pragmas can lead to significantly different FPGA performance. Table 9 shows the latency (clock cycle) of each target kernel’s best pragma design and worst pragma design in our dataset. The shorter latency the better. We also list the mean and standard deviation of latency in our dataset, and the latency of not inserting any pragma. We can see that the gap between the best design and worst design is very big, and the worst design is sometimes even worse than not inserting any pragma. This is because some pragmas might use too many resources and occupy the resources of other modules. The standard deviation is also very large, and sometimes it is even larger than the mean. Therefore, the pragma design is very difficult.

Additional Problem Analysis Challenges of Domain Shift

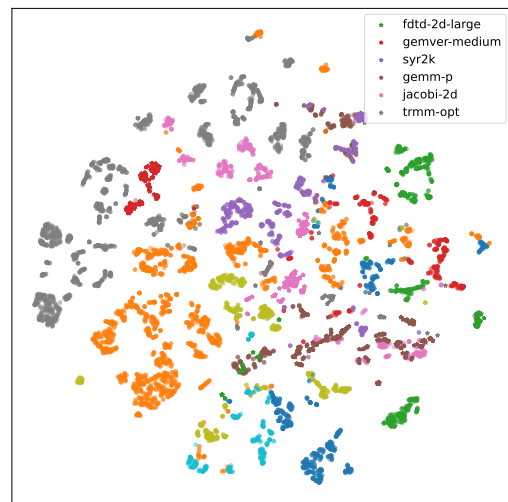


Figure 4: Visualization of the graph embeddings. Each point is a pragma design. Points belonging to the same kernel have the same color. Points from the same kernel are clustered together, while points from different kernels are located in different places. Due to the limited number of colors, different kernels might use the same color. Due to the limited space, we only show the names of the target kernels.

Domain shift brings a lot of challenges to our task. First, as shown in Table 9, the mean latency of different kernels is very different, and we hope the model can learn this distribution, so we cannot align the representation space of different kernels, as did in many previous domain generalization papers. We extract the graph representation of each design point from the HARP model and visualize it in Figure 4. In the figures, points belonging to the same kernel have the

Table 9: The latency (clock cycle) of each target kernel’s best pragma design and worst pragma design in our dataset. We also list the mean and standard deviation of latency in our dataset, and the latency of not inserting any pragma.

	Fdtd-2d-large	Gemver-medium	Syr2k	Gemm-p	Jacobi-2d	Trmm-opt
Best design	2,355,778	210,335	46,061	9,179	164,284	9,387
Worst design	96,496,392	1,826,012	2,005,329	2,110,866	5,520,201	1,547,247
Mean	27,529,638+-37,088,252	644,066+-313,804	170,139+-353,609	135,877+-251,531	3,049,134+-1,544,708	329,745+-347,427
No pragma	14,362,849	1,826,012	533,981	461,231	625,124	1,547,247

same color. Due to the limited number of colors, different kernels might use the same color. We can see that points from the same kernels are clustered together, while points from different kernels are located in different places. The visualization further verifies that the domain difference between different kernels is very big. Such a big difference is informative to the model, so we cannot align the representation space of different kernels.

```

for (j = 0; j < 80; j++) {
  if (j <= i) {
    C[i][j] += alpha * A[i][k] * A[j][k];
  }
}

```

Figure 5: Code snippet of the “syrk” kernel. The line inside this nested loop is the only difference between the “syr2k” kernel and the “syrk” kernel. However, their best pragma designs are very different.

Second, kernels share some similar substructions, where both their similarities and differences should be carefully noticed. The similarity could benefit the MoE model by utilizing the knowledge learned from other kernels. Nonetheless, the difference is also very important. An example is the “syr2k” kernel and the “syrk” kernel. They only differ in one line inside a nested loop, shown in Figure 5 and Figure 3. However, their best pragma designs are very different. In the best pragma design of “syrk”, the tiling factor of “_TILE_L2” is 60, but it is 1 for “syr2k”; the parallel factor of “_PARA_L1” and “_PARA_L2” are 20 and 1 for “syrk”, but they are 8 and 4 for “syr2k”; “syrk” uses coarse-grained pipeline for “_PIPE_L2”, but “syr2k” does not use pipeline there. Therefore, domain generalization is difficult for HLS prediction models. The MoE structure can utilize similar experts to deal with similarities, but it can also discern the differences and use different experts to deal with them.

HARP Model Illustration

Figure 6 illustrates the HARP model using the same diagram style as our model’s diagram (Figre 2 in the main paper). It shows the five components of the HARP model. Since we focus more on the MoE structure, the diagram ignores some details of the HARP model. For more details, please refer to the HARP paper (Sohrabzadeh et al. 2023).

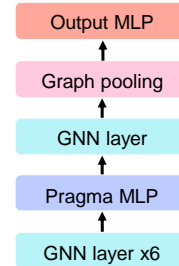


Figure 6: HARP model diagram.

Detailed Experiment Settings

Datasets. The HLSyn benchmark dataset (Bai et al. 2023) consists of 42 kernels selected from the MachSuite dataset (Reagen et al. 2014) and the Polyhedral dataset (PolyBench) (Pouchet 2012). Since the FPGA’s latency is too diverse, it is difficult for the model to directly learn. Thus, we normalize the FPGA’s latency by $0.5 * \log_2(\frac{1e7}{\text{latency}})$ as the normalized performance. It is the lower the better for the original latency, but it is the higher the better for the normalized performance. Our HLS targets the Xilinx Alveo U200 FPGA with a working frequency of 250MHz. We also normalize the resource utilization by dividing it by the total available resources of the targeting FPGA. We mainly care about four types of resources: LUT, FF, DSP, and BRAM, so we have five prediction targets including the normalized performance.

Our resource constraint is that each resource type should be used no more than 80%, because we need to leave some spaces for downstream tasks or other additional modules. We hope the model can make accurate predictions of the performance and resource utilization, so we can search for the best pragma design that satisfies the resource constraints and has the best normalized performance (lowest latency). We rely on the classification model to help us wipe out the invalid designs, but we rely on the regression model to help us wipe out the valid designs that exceed our resource constraints.

Evaluation. We use 80% of data points in the source kernels as the training set to pre-train the model, 10% for validation, and 10% for testing. We use five random seeds (1, 2, 3, 4, 5) to randomly split the source kernel’s dataset. The MSE on the source kernels is unimportant, so currently the test set on the training kernels is not used. We use the validation set for early stopping. We pretrain the model for 1000 epochs, then we finetune it for 500 epochs on the target kernels. During fine-tuning, we use the same random seed as

used in that model’s pretraining. We run offline evaluation five times. For online evaluation, since HLS takes a long time, we use the three models trained with random seeds 1, 2, and 3 to run HLS. In offline evaluation, we calculate the sum of the MSE of the five prediction targets. In online evaluation, from the designs that are predicted to be valid and under resource constraints, we pick the top 10 designs with the lowest predicted latencies to run HLS. When running HLS, we set the timeout as 3 hours. If the HLS does not finish within 3 hours, it is very likely to be unsynthesizable, so we will terminate the HLS and treat it as an invalid design. We calculate the mean speedup of the three repeated HLS experiments for each target kernel. Then we calculate the mean speedup or geometric mean speedup for all target kernels.

MoE on various granularities in a single model. In the experiments section in the main paper, we conduct an experiment of applying MoE on various granularities in a single model (Table 3 in the main paper). When we utilize the block MoE and the graph MoE together, or the node MoE and the graph MoE together, there is no conflict and we can smoothly apply them. However, when we utilize node MoE and block MoE together, or when we utilize MoE on all three granularities, we face a conflict. The block MoE model removes the GNN layer after the pragma MLP, but the node MoE is applied to that GNN layer. Therefore, we slightly modify the model structure to accommodate both models. We keep that GNN layer after the pragma MLP and apply MoE on it, as the node MoE. After it, we follow the paradigm of the block MoE model: adding an additional block MoE layer for pseudo nodes after that GNN layer, and we do graph pooling only on pseudo nodes. We can further apply graph MoE on the output MLP. In this way, we allow MoE on both node and block granularity, or on all three granularities.

Baseline methods. For all baseline methods, we follow their original best hyper-parameter settings. For our models, we follow the same hyper-parameter setting and training strategy as HARP, except for the MoE’s unique hyper-parameters. We will specify the hyper-parameters in a later section.

- HARP: we use its original settings and official codes (<https://github.com/UCLA-VAST/HARP>).
- HARP+MAML: we use MAML to help find a good initialization for HARP model’s parameters based on the source kernels. Then we use the normal fine-tuning strategy for it on the target kernels. We use the implementation of the “learn2learn” Python package. We randomly sample 32 kernels with replacement per epoch to train.
- ProgSG: it uses both text embedding of the source code and the ProGraML graph as the input. We use its official codes (<https://github.com/zongyueqin/progsg>).

Supplementary Experiment Results

Study of Model Variants

As analyzed in the Experiments section in the main paper, one concern is whether the hierarchical MoE model simply

benefits from having more parameters. To address this concern, we enlarge the hidden size of HARP from 64 to 128 and 256, and we evaluate their performance. The results are listed in Table 10. As we enlarge the hidden size, the MSE also increases. Even if the parameter size is larger than hierarchical MoE, its performance is still worse than hierarchical MoE. In the original best hyper-parameter setting of HARP, 64 is already the best-performing hidden size. We also list the parameter size of single-level MoE models in Table 11. If we do not utilize the hierarchical structure, only using MoE on one granularity does not significantly increase the parameter size. It verifies that parameter size is not the key reason for MoE’s success.

Table 10: Influence of the model’s parameter size. “#Param” indicates the parameter size.

Model	Hidden size	#Param	MSE
HARP	64	359,370	0.202
	128	1,053,610	0.240
	256	3,445,130	0.327
Hierarchical MoE	64	1,329,403	0.143

Table 11: Parameter size of the single-level MoE models that do not have the hierarchical structure.

	Node MoE	Block MoE	Graph MoE
#Param	473,870	361,805	431,901

Another concern is about the number of experts. In the hierarchical MoE, if we only utilize MoE on the node granularity or graph granularity, its performance is slightly worse than utilizing MoE on three granularities, but it could still perform well (Table 4 in the main paper). In this case, the three expert models for the high-level MoE have the same structure. Each of the low-level MoE models has 4 experts, so in total we have 12 experts for that granularity and 3 experts for other layers that are not equipped with low-level MoE. Does its success come from a large number of expert models (12 experts for that granularity), or the hierarchical structure (12 experts for that granularity + 3 experts for other layers)? To answer this question, we run experiments on the single-level MoE structure with different numbers of experts. In addition to our original setting using 4 experts, we experiment with 2, 8, and 12 experts. The results are listed in Table 12. Increasing the number of experts does not necessarily improve the performance. For all three MoEs, the lowest MSE is achieved when we use 4 experts. Therefore, the performance gain is probably because of the hierarchical structure (12 experts for that granularity and 3 experts for other layers).

As discussed in the main paper, when we were designing the block MoE’s structure, there were many design choices, from which we chose the current one. We also conduct experiments on other variants of the single-level block MoE model. In our design, we remove the GNN layer after the

Table 12: Influence of the number of experts in the single-level MoE model. The listed results are test MSE. We use **bold** to mark the best number of experts for each model.

Model	2 experts	4 experts	8 experts	12 experts
Node MoE	0.160	0.160	0.302	0.195
Block MoE	0.208	0.171	0.207	0.264
Graph MoE	0.305	0.216	0.229	0.229

pragma MLP, and we remove the graph pooling on the normal nodes. Therefore, we only rely on the pseudo nodes after the GNN encoder. This is because the pseudo nodes are sufficient for making the final prediction after we add the block MoE layer. Here we preserve the GNN layer after the pragma MLP, or preserve both the GNN layer and the graph pooling on normal nodes. The results are shown in Table 13. Our design archives the lowest MSE. It verifies the effectiveness of our design.

Table 13: Variants of the single-level block MoE model. “Block MoE+GNN” means we preserve the GNN layer after the pragma MLP in the block MoE model. “Block MoE+GNN+pooling” means we preserve the GNN layer after the pragma MLP and the graph pooling on normal nodes in the block MoE model.

	Block MoE	Block MoE+GNN	Block MoE+GNN+pooling
MSE	0.171	0.529	0.240

Analysis of Expert Assignment

Due to the limited space, we only analyze the gating network of the high-level MoE and the block MoE in the main paper. Here we analyze the gating network of the node MoE and the graph MoE. We still pick the best-performing hierarchical MoE model from the five repeated experiments to analyze. For the node MoE, we show the averaged assigned weights for each type of node in Table 14. There are three non-overlapping types of nodes: normal nodes that represent the data and instructions, pseudo nodes that represent basic blocks, and pragma nodes that represent pragmas. A special type of normal node is icmp node, which represents the “icmp” instruction of a loop. If a pragma modifies a loop, that pragma node will be connected to both the icmp node and the pseudo node corresponding to the loop, so the icmp nodes are very meaningful. The normal nodes and pseudo nodes are relatively equally distributed to the experts. The icmp nodes are mainly handled by the third expert, and the pragma nodes are mainly handled by the fourth expert. Similar to our analysis of the block MoE in the main paper, the node MoE’s experts also diversify their roles.

For graph MoE, based on the expert assignment weights of each data point, we calculate the average expert assignment weights of each kernel. Then, we can calculate the cosine similarity between two kernels using the weights. Table 15 lists the most similar source kernel of each target kernel. “Gemver-medium” and its most similar ker-

Table 14: Average assigned weights of the node MoE. Each column shows the expert weights for a certain type of node. There are three non-overlapping types of nodes: normal nodes, pseudo nodes (basic block), and pragma nodes.

Expert	Normal	Icmp (\in normal)	Pragma	Pseudo
1	25%	0%	25%	30%
2	23%	31%	0%	27%
3	27%	69%	10%	11%
4	25%	0%	65%	32%

nel, “gesummv-medium”, are both matrix-vector multiplications; “syr2k” and its most similar kernel, “syrk”, are both symmetric rank operations; “trmm-opt” and its most similar kernel, “symm”, are both matrix multiplications. This indicates that the expert weights assigned by the graph MoE are partially explainable.

Other Detailed Information

Hyper-parameters. We basically follow the hyper-parameter settings of HARP. We use the Adam optimizer to train the model for 1000 epochs and fine-tune it for 500 epochs. The learning rate is $1e-3$ and the weight decay is $1e-4$. We use the cosine annealing learning rate schedule (Loshchilov and Hutter 2017) with a minimum learning rate of $1e-5$, and the unturned linear warmup (Ma and Yarats 2021). We set the hidden size as 64 and the dropout as 0.1. The regression models use the MSE loss to train, while the classification models use the cross entropy loss. In the first design of the high-level gating network, we use the graph pooling of input features (Equation 5 in the main paper). Its MLP has two layers and one ReLU function between them, where the first layer has the same hidden size as the input dimension and the second one shrinks the output dimension to 1.

For hyper-parameters related to MoE, we try the hyper-parameters in a reasonable scope and use the best one with the lowest test MSE on the target kernels. The low-level MoE uses the weighted sum of 4 experts, and the high-level MoE calculates the weighted sum of three models (the node MoE model, the block MoE model, and the graph MoE model). The gating network is a linear layer and a softmax function. We set the weight of the regularization term of MoE, both α and β , as $5e-3$. In the two-stage training of the high-level MoE, the first stage (warmup) takes the first 500 epochs, and the second stage takes the later 500 epochs. In the model variants experiments, we only modify the different parts as introduced in the experiments. Table 16 lists the scope of hyper-parameters we have tried.

Reproducibility. We have submitted our data and codes in the supplementary material. The readme file contains instructions on how to run the codes. We have introduced the important hyper-parameters in this appendix, while other hyper-parameters can be found in the “src/config.py”, We use NVIDIA L40S (40GB) to train our model. It takes about 5 hours to train the model on the source kernels and about 1 hour to fine-tune on the target kernels. Training costs about

Table 15: The most similar source kernel of each target kernel based on the graph MoE’s expert assignment weights.

Target kernel	Domain	Source kernel	Source domain
fdtd-2d-large	2-D finite different time domain kernel	bicg-large	BiCG sub kernel of BiCGStab linear solver
gemver-medium	matrix-vector multiplication	gesummv-medium	matrix-vector multiplication
syr2k	symmetric rank-2k operations	syrk	symmetric rank-k operations
gemm-p	matrix multiplication	covariance	covariance computation
jacobi-2d	2-D Jacobi stencil operations	doitgen-red	multiresolution analysis
trmm-opt	triangular matrix multiplication	symm	symmetric matrix multiplication

Table 16: The scope of MoE-related hyper-parameters that we have tried. “Choice” is our final choice.

Hyper-parameter	Scope	Choice
Number of experts	2, 4, 8, 12	4
Number of used experts	2, 4, 8, 12	4
Regularization term α	5e-4, 1e-3, 5e-3, 1e-2	5e-3
Regularization term β	5e-4, 1e-3, 5e-3, 1e-2	5e-3
Fine-tuning epochs	300, 500, 700	500
Node MoE’s place	every layer in the GNN encoder, the GNN layer after pragma MLP*, additional linear layer	marked
Block MoE’s place	pragma MLP, pooling, additional linear layer, additional linear layer and remove some layers*	marked

30 GB of memory and fine-tuning costs about 12 GB of memory. Now we load the whole dataset into the memory before training. If the memory is not sufficient, we have an argument to disable this feature conveniently, and the memory cost for training can be reduced to about 15 GB. We run HLS on an AMD EPYC 7V13 64-core processor. We run HLS for the selected top-10 design points in parallel. It takes about 10 CPUs, 50 GB of memory, and 3 hours to run 10 design points for one kernel.

Limitations and Future Work

Though we have made much progress on domain generalization for HLS prediction, we also face many limitations. First, the hierarchical MoE model does not have a huge advantage over HARP on every kernel. As shown in Table 1 in the main paper, it is significantly better than HARP on “Fd” and “Gemv”, slightly better on “Gemm” and “Tr”, but it is the same as HARP or worse than HARP on “Sy” and “Ja”. This might be due to the inherent difficulty of this problem. Future research is needed to develop even stronger models.

Besides, the hierarchical MoE structure is mainly useful in quick domain adaption using a small amount of data to fine-tune. However, when the computing resource is abundant enough to run a lot of HLS on the target kernels, we will have more data points for fine-tuning, and in this case, MoE would perform similarly to HARP. The proposed model should be used in suitable applications. It also remains an open question of how to enhance the model’s general ability when the data is abundant.